

Impact of Large Offshore Wind Farms on Power System Transient Stability

F. Shewarega, *Member, IEEE* and I. Erlich, *Senior Member, IEEE*, José L. Rueda, *Student Member*.

Abstract— This paper deals with the impact of large scale wind power integration on the transient stability performance of power systems. Typical offshore wind farm topologies including the medium and high voltage submarine cables, the generator, the multi-stage transformers, the controllers were simulated using real-world values. Voltage and power at the point of common coupling and the swing curves of conventional synchronous generators following a major grid fault were computed and the critical fault clearing times were determined and compared with one another for different levels of wind integration. It was found out that using the currently established controller structure and parameter settings, the transient stability performance of the system deteriorates with increasing wind integration. The study has also revealed that there are a range of options to improve the performance of the system even to the extent of improving on the performance of the system beyond the baseline scenario where there is no wind power generation at all.

Index Terms—Doubly-fed induction machine, wind generator control, transient stability, wind power.

I. INTRODUCTION

THE installed wind generation capacity has continued to increase worldwide at a fast-paced rate. As of this writing the total capacity in Germany has surpassed the 23-GW mark, putting Germany well on target to meet the projected 50 GW wind capacity by the year 2020. In most European countries where wind power has taken significant strides, the onshore sites have now been exhausted and the expected expansion is set to take place offshore. A significant amount of offshore capacity has already been connected to the European grid. Others with capacities ranging in hundreds of megawatts are being built and are in the process of coming online. Whilst onshore wind turbines were connected to the medium voltage network, the upcoming offshore farms will all be connected to the 400-kV network.

Extrapolating the current trend into the future, it is easy to foresee installed wind capacities exceeding 50 % of the overall capacity in some countries in the not too distant future. With increasing wind power generation, interest to fully understand and quantify the impact of this development on the performance of the interconnected system has also grown. While individual onshore wind units in the past were only required to maintain a prescribed power factor range at the point of interconnection, now transmission system operators (TSO) are putting more wide-ranging conditions. Some TSO have issued grid codes spelling out a range of operational requirements, which wind farms need to fulfill upon connection to the grid. These include low voltage fault

ride-through capability and voltage support following grid faults. Requirements concerning additional ancillary services are also likely to follow. It should also be borne in mind that the control systems which modern wind turbines employ are characterized by fast response time and thus open up additional, unconventional options to help meet these requirements.

The objective of this paper is to investigate the effect of wind turbines on the transient stability of conventional synchronous generator units operating on the system and explore some of the possible control measures that can help stabilize the system in the post fault scenario. Wind based generation systems and conventional synchronous generators exhibit fundamentally different transient responses. This stems first and foremost from their inherently different dynamic characteristics. Additionally, wind generation systems result in the reduction of the overall system inertia pegged to the network in relation to the installed capacity. As a rule, wind power is dispatched on a priority basis irrespective of its merit order. In countries with widespread and expansive wind installations the resulting shift in load flow configuration can adversely impact the transient stability performance of the entire system. This topic, however, is not going to be the focus of this study since the problem presupposes the knowledge of the topology of the actual network to be studied.

The transient stability problem in the sense that one or a group of generators may be forced out of synchronism following a grid fault does not as such apply to wind power generation systems. In critical situations, the converters can be stopped for duration of a few milliseconds and then resynchronized. The role of the inertial response, which is so central to the behavior of conventional synchronous generators following a disturbance, is largely supplanted by the response of the controllers in wind generation systems. The study of the impact of the wind generation plants and the quality of the results obtained thus relies to a large extent on the quality of the models of the control systems and the accuracy of the parameters. As part of the research for this paper, real-world parameters and values for the DFIG and its control systems, for the transformers and the submarine cables have been put together in appendix. These parameters are not necessarily attributable to a particular manufacturer or brand but can be considered representative values for megawatt level turbines in use today.

The paper is structured as follows. The section following this introduction will describe the test network and the

methodology to be used for the study. This will be followed by the review of the models used for wind generation system and the other components of the grid for transient stability study. Finally some simulation results will be presented, which will then be followed by discussion of the results and some conclusions.

II. MODELLING APPROACH

A. Test Power System and Methodology of Investigation

The test network given in Fig. 1 has been used for this study. All the relevant data for the network and its components are summarized in appendices 1 – 3. For a fault at the location indicated in the figure the critical clearing time with only conventional synchronous generators in operation is around 260 ms.

The methodology adopted for characterising the effect of increased wind power generation on the transient stability behaviour of the system and deducing conclusions which may reveal possible counter measures was to replace in stages each of the 400-MW conventional generations plants with wind units of similar combined capacity. Thereby the system including the internal medium voltage network of the wind farm, the submarine cables, the multi-stage transformers were simulated using real-world values. A typical arrangement for incorporating offshore wind farms to the grid that was used in this study is given in Fig. 2. Additionally, the power (real as well as reactive) injected into the PCC is maintained at exactly the same value for each level of wind power integration (20 – 100%). The submarine cable linking up the wind farm to the PCC at an onshore location comprises of two parallel cables. The charging reactive power of the cables is compensated using shunt reactors connected directly to the four cable terminations. To avoid any unintended de-energization of the cables without the compensation reactors (to avoid problems arising from the interruption of a capacitive current), both the cables and reactors are switched concurrently using the same switch. The reactor on the onshore side is continuously adjustable in the range of 40 – 100% (the onshore side is chosen for control in practice on grounds of ease of operation). The wind turbines themselves are assumed to be producing no reactive power during normal operation and the reactive power reference is set zero. To meet the reactive power requirements as specified in the grid code additional capacitances are installed, which are also variable.

B. Wind Turbine Modelling

By far the larger number of wind generation plants at this point in time are still equipped with the doubly-fed induction generator (DFIG). As a result, this paper focuses on this type of machine only. As is well known, the rotor terminals of a DFIG are fed with a symmetrical three-phase voltage of variable frequency and amplitude fed through a voltage source converter usually equipped with IGBT based power electronic circuitry [1], [2]. The basic topology including its control

system is shown in Fig. 3.

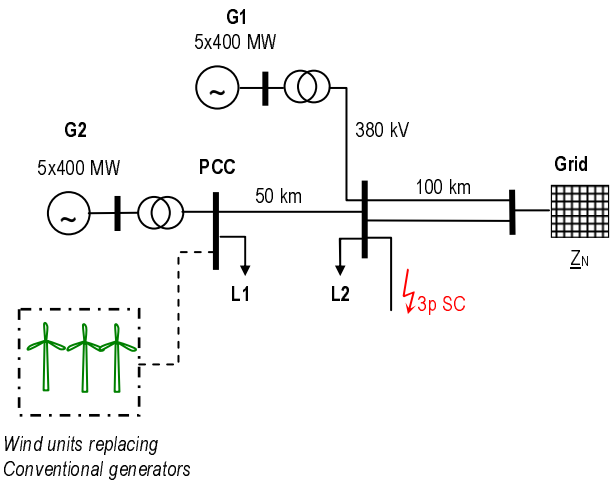


Fig. 1. Two-area, weakly coupled test network.

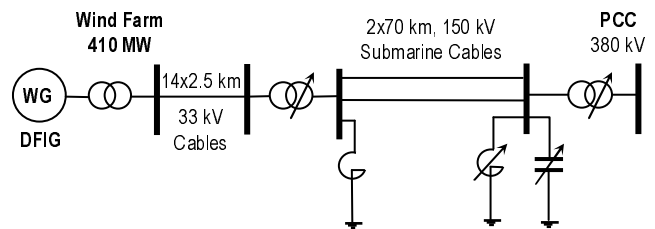


Fig. 2. Connection of offshore wind park to the grid.

The modeling of the induction machine in and of itself is dealt with in numerous papers and textbooks and can be considered basic. As a general approach, the space-phasor coordinates with orthogonal direct (d) and quadrature (q) axis is used. The choice of the stator voltage as the reference frame enables the decoupled control of P (d control channel) and Q (q control channel).

The two complex (i.e. complex in terms of space-phasor representation) voltage differential equations, one each for the stator and rotor circuits, together with the equation of motion represent the full set of mathematical relationships that describe the dynamic behavior of the machine [3], [4]. Then, by setting the derivative of the stator flux linkage with respect to time to zero, the quasi stationary model of the machine, given in Fig. 4, is obtained

A complete model of the DFIG also includes models of the real and reactive power control together with speed and pitch angle control. These models, however, are not relevant for the purposes of this study, which is synchronism of generators in conventional plants following a fault. The structures of both the rotor side controller (RSC) and line side controller (LSC) are given in Fig. 5 and Fig. 6, respectively. The two figures summarize the models of the core functionalities of the systems, which are of relevance for stability studies. Manufacturers often augment these core structures variously. The structures as presented here reproduce neither any eventual blocking of the converters nor crowbar activation

during grid faults. Additionally, due to the assumption that the DC voltage can be maintained approximately constant during the simulation time span models of the DC link and the crowbar are not needed. The air gap torque of the machine is also assumed to remain constant.

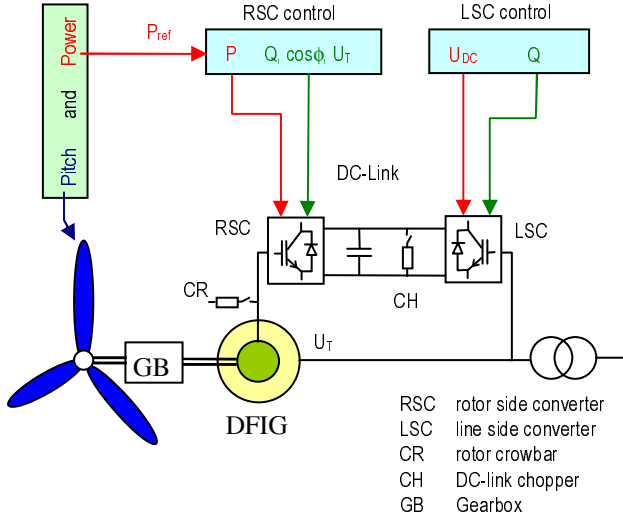


Fig. 3. Layout of DFIG based wind turbines.

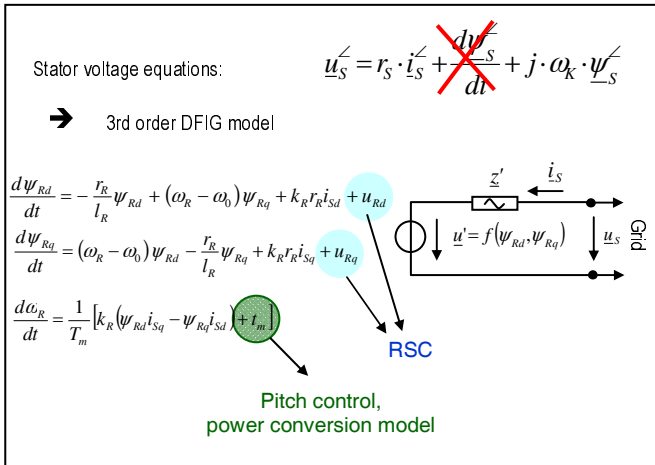


Fig. 4. Reduced 3rd order DFIG model.

The voltage controller in Fig. 5 maintains a deadband of $\pm 5\%$ to preclude controller action until the voltage exits this limit. As per the German grid code, for onshore wind farms the deadband is set at $\pm 10\%$ while for offshore plants the deadband is $\pm 5\%$. According to this grid code [5], on either end of the deadband the reactive current reference (in response to the voltage deviation) makes a sudden jump and then goes on to increase/decrease in relation to the voltage deviation. In the model used in this paper, however, the rise takes place linearly without an initial jump (comparison shown in Fig. 5). The issue of deadband and more generally the type of the voltage controller to be used, as will be shown later in this paper, has a significant bearing on the transient stability behaviour of the system. It should also be reminded that representative values for controller parameters are given

in the appendix.

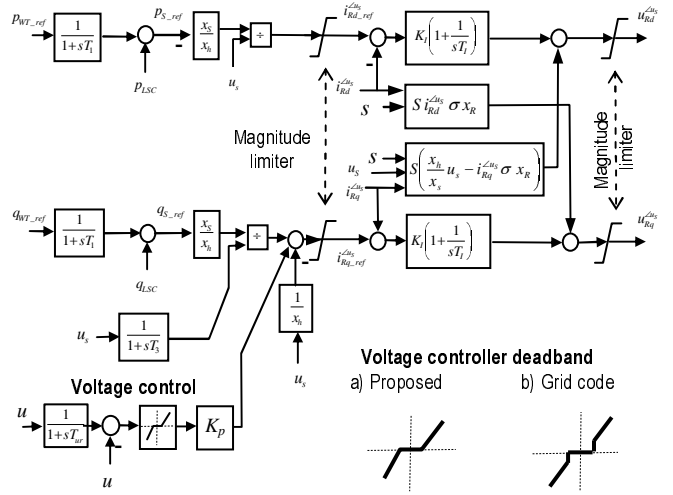


Fig. 5. Rotor side converter model.

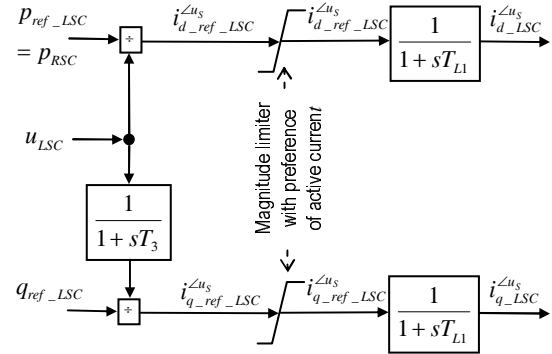


Fig. 6. Line side converter model.

III. SIMULATION RESULTS

A. Basic differences between conventional generation plants and wind turbines

As a baseline case, the response in terms of real and reactive power together with voltage at the PCC of conventional synchronous generators to a grid fault of 260 ms duration is shown in Fig. 7. For comparison, the time variation of these same variables when the conventional synchronous generators in G2 are completely replaced by the DFIG using commonly used voltage control approaches, which include proportional controller and a deadband of $\pm 5\%$, is shown in Fig. 8.

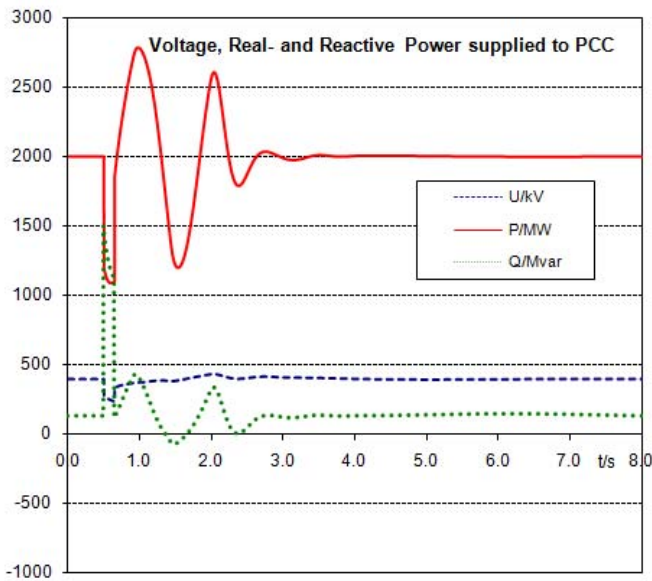


Fig. 7. Response of 2000-MW conventional power plant to a grid fault.

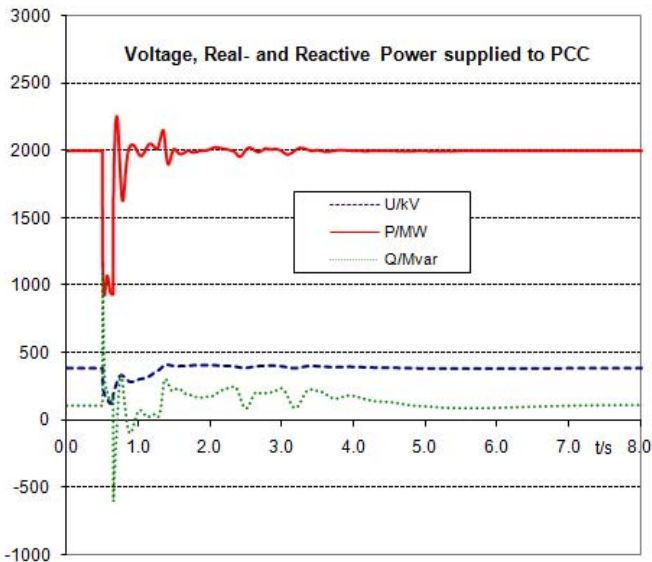


Fig. 8. Response of 2000-MW wind farm with wind turbines equipped with proportional voltage controller (5% deadband, 2.5 p.u. gain) to a grid fault.

The first observation that stands out is the electromechanical power swing that the conventional synchronous generators experience as opposed to wind turbines where only much smaller ripples excited by the controllers occur. As a result, in the DFIG the real power quickly settles at the pre-fault value. It can also be observed from the comparison of the two plots the fact that during the fault conventional synchronous generators are capable of supplying a significantly larger reactive power than before to support the voltage. The reactive power in-feed by the DFIG at the PCC during this phase is limited. It can thus be concluded that although the DFIG is capable of restoring its real power output quickly to the pre-fault value following the fault clearance - crucially as far as the transient stability

performance of the whole system is concerned - the reactive power support by the wind turbines at PCC is limited. This is confirmed by the power angle swing curves of generators G1 and G2 (Fig. 9), where the maximum swing angles increase with the share of wind. It can thus be surmised that the larger the share of wind power generation, the worse the transient stability performance of conventional generators. This assumption is further re-inforced by Fig. 13, which shows, in the absence of additional measures, the critical fault clearing time decreases as the share of wind power generation increases.

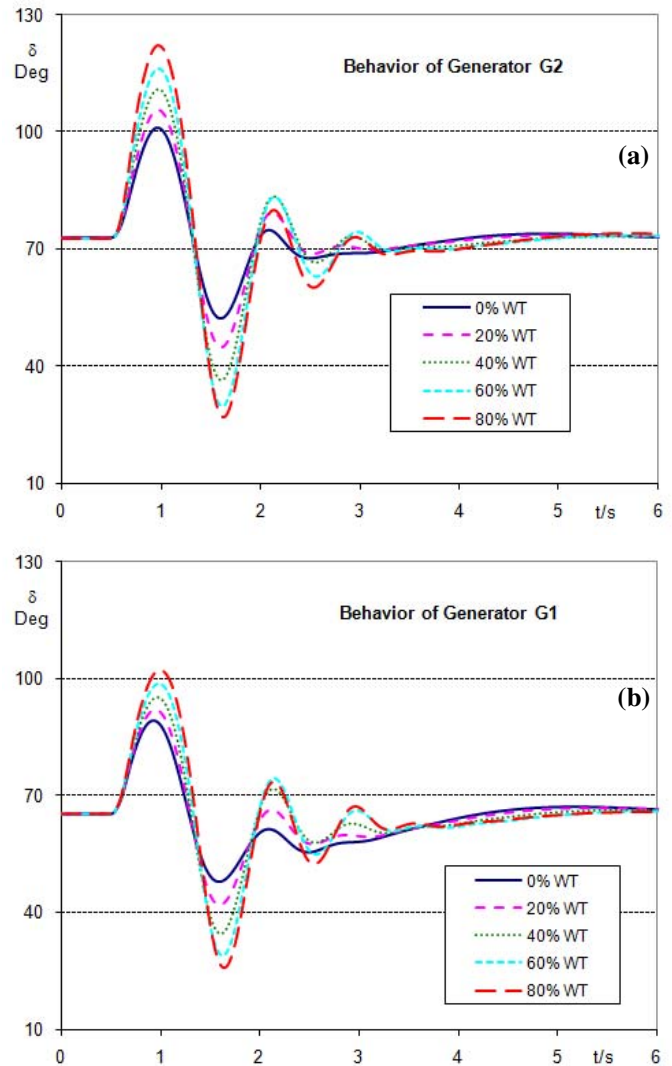


Fig. 9. Effect of wind based power generation on the power angle swing curve.

B. Impact of the deadband and increased proportional gain of DFIG voltage controller

In Fig. 10 the same scenario, but without the dead band, i.e. with the voltage being continuously controlled however small the magnitude of the deviation may be, is simulated. It can be observed by comparing these plots with Fig. 8 that oscillations in real and reactive power as well as in the voltage are significantly reduced. But the low reactive power output

during the fault remains unchanged. In Fig. 11, the removal of the deadband has been augmented by an increase in the proportional gain to 7.5. (Please note that the minimum proportional gain prescribed by the German grid code is 2.0.) The figure shows that not only the power oscillations are almost entirely eliminated but also the wind turbine is now capable of voltage support by providing reactive power comparable in magnitude to that of the synchronous generators. It can thus be concluded that as far as the transient stability performance of the system is concerned wind power performance can be significantly enhanced by increasing the proportional gain and discarding the deadband of DFIG voltage controller. This conclusion is further underlined by the change in the critical fault clearing time that can be achieved (Fig. 12 and Fig. 13). The merit or demerit of this measure in the broader context remains to be investigated. But it can in point of fact be stated that continuous voltage control without a deadband and increasing the voltage controller gain is one of the available options to improve the transient stability behaviour of the system.

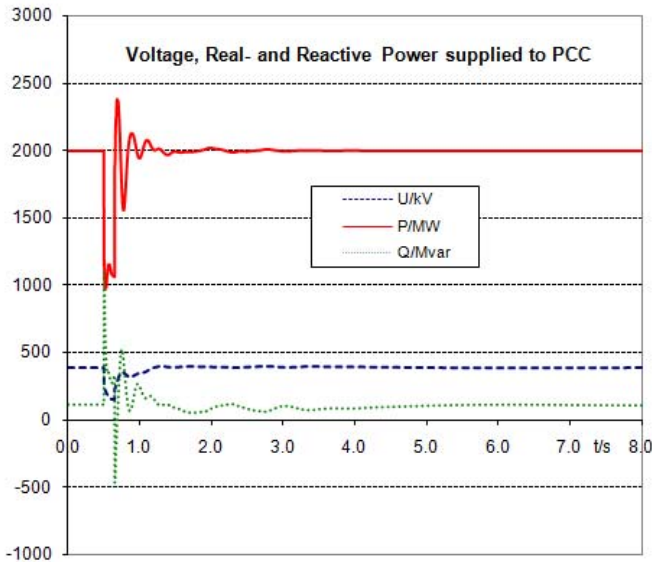


Fig. 10. Response of 2000-MW wind farm with wind turbines equipped with proportional voltage controller without deadband and 2.5 p.u. gain to a grid fault.

C. Effect of wind farm size on transient stability performance

In the simulations up to this point, the conventional generators were replaced by wind turbines of comparable installed capacity. This, however, does not tally with the reality. The output power of a wind farm rarely reaches the combined installed capacity of its units. More likely in practice is a much larger installed capacity and the wind farm operating in part-load mode. To take account of this fact, the installed capacity of the wind turbines replacing conventional plants was assumed to be 50 % higher than the rating of the conventional plants they are replacing. With the increase in the installed capacity an additional cable was added to the two parallel 150-kV cables, the transformer ratings were increased

accordingly, the 14 pieces of 33-kV cables were increased to 21 and the compensation reactors were also adjusted correspondingly.

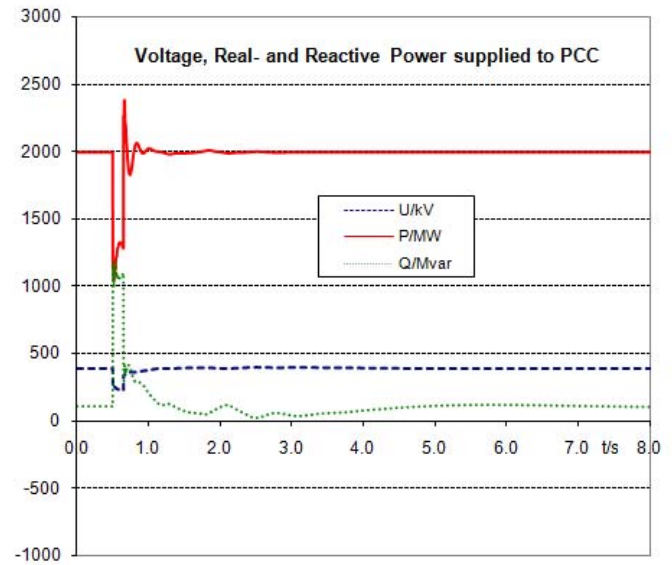


Fig. 11. Response of 2000-MW wind farm with wind turbines equipped with proportional voltage control without deadband and 7.5 p.u. gain to a grid fault.

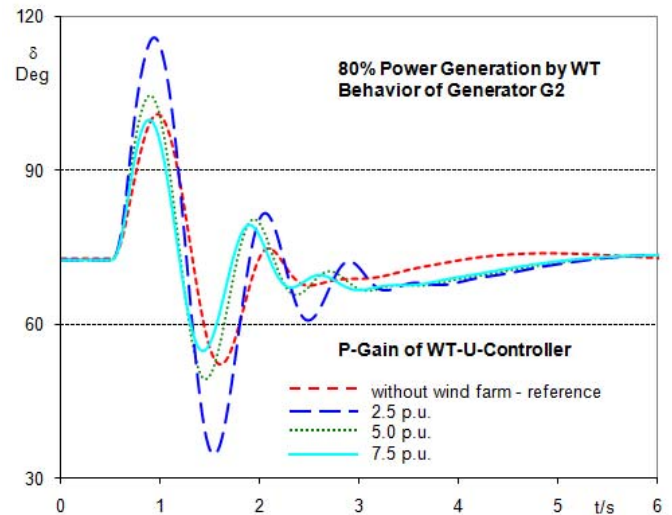


Fig. 12. Effect of proportional gain on maximum swing angle.

As observed in Fig. 10, wind turbines possess limited capability to inject reactive power into the PCC to support the voltage during short-circuit. As long as the magnitude limit is not reached, the reference values for the real and reactive current of the DFIG are determined by the superordinate controller, otherwise the real current reference is reduced to remain within limit. With the capacity increased by 50 %, it would appear that the wind farm now possesses a correspondingly larger leeway to increase the reactive current and thus support the voltage at PCC more effectively.

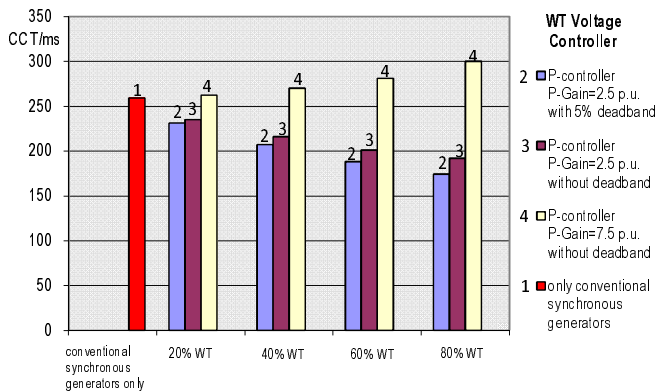


Fig. 13. Effect of Controller options on critical fault clearing time (CCT)

To study and quantify the effect of increased installed capacity, the conventional synchronous generators in G2 were fully replaced by wind turbines, but, as opposed to the simulations in the previous sections, the installed capacity of the wind turbines has now been increased by 50 % to 3525 MVA. (Please also note that in terms of load flow the pre-fault conditions are identical for both installed capacities.) As expected the active and reactive currents injected into PCC increase with the increased capacity of the wind farm (Fig. 14 (c) and (d)). But against expectations, the increased reactive power injection does not translate into increased voltage support. In fact the voltage at PCC decreases with the increase in installed wind capacity (Fig. 14 (b)). This fact is further underscored by Fig. 14 (a), which shows that the maximum swing angle for the generators still in operation (G1) is greater than it was for lower installed capacity.

To elucidate why an increase in installed capacity adversely impacts the voltage at the PCC, the link between the wind farm and the PCC was modeled using a series impedance as shown in Fig. 15. With the reactive current maintained at 1.0 p.u., the effect of the active current on the voltage drop on the link in relation to the R/X ratio of the series impedance is plotted in Fig. 16. This simple illustration reveals that, depending on the R/X ratio of the link, the real and reactive currents can work at cross-purposes in terms of supporting the voltage at PCC. In other words, for practically occurring R/X ratios in excess of 0.25 the voltage boosting effect of the reactive current can be offset by the real current.

As a possible solution for overcoming this effect and more generally for reducing the adverse effect of the real current on voltage during fault, a voltage-dependent active current control (VACC) is proposed. The approach involves modifying the active power reference in accordance with (1).

$$I_{active_ref}^* = F^2 I_{active_ref} \quad (1)$$

The factor F in (1) is computed as shown in Fig. 17, which is inserted as an upstream block into the active current controller.

The insensitivity range lapses at 90 % of the steady state voltage, below which point the active current reference is reduced. This will obviously have a load-relieving impact on

the machine and thus increase the mechanical speed of the turbine during the fault. Under circumstances the speed limit may put a check on the use of the method, but until the limit is reached it proves to be effective as shown in Fig. 18. Not only that the swing curves are now almost identical but also the maximum angle is reduced compared even to the more favorable case in Fig. 14 (a).

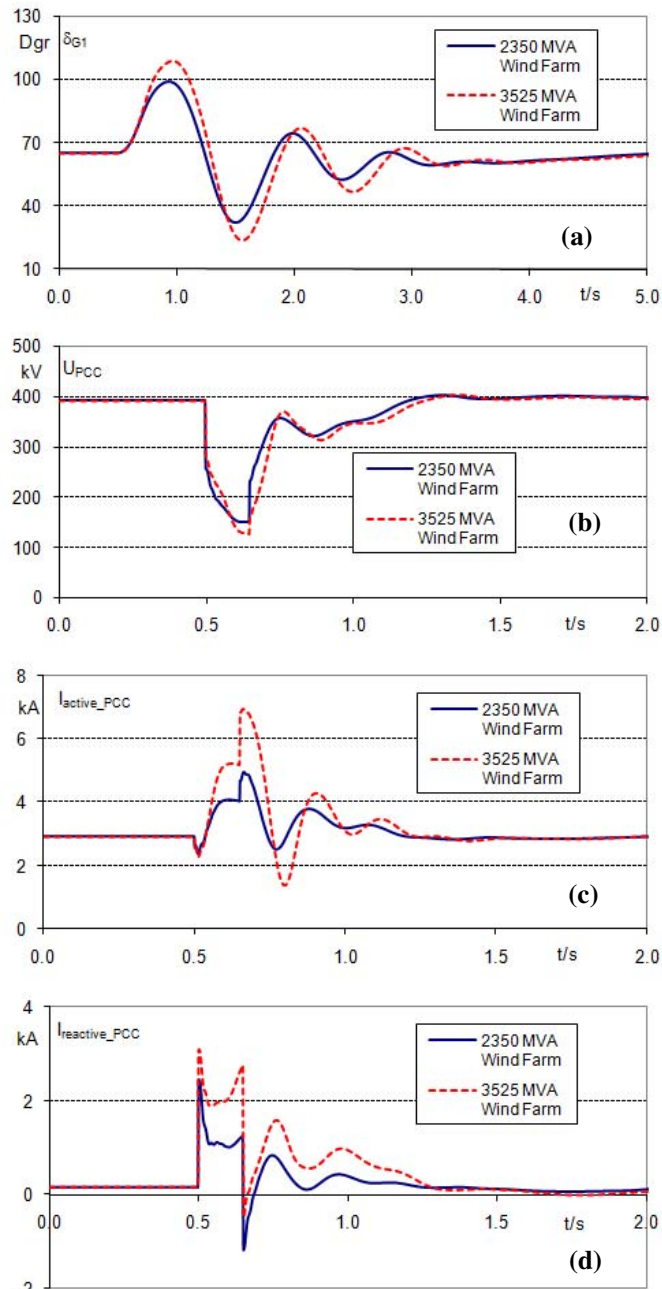


Fig. 14. Comparison of the performances of wind farms of different size.

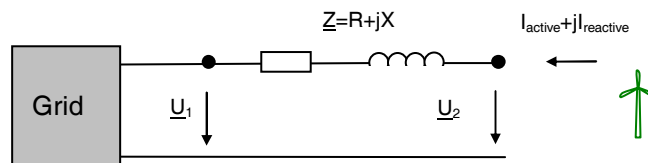


Fig. 15. Simplified circuit for the investigation of the effect of real and reactive current injection by wind turbines.

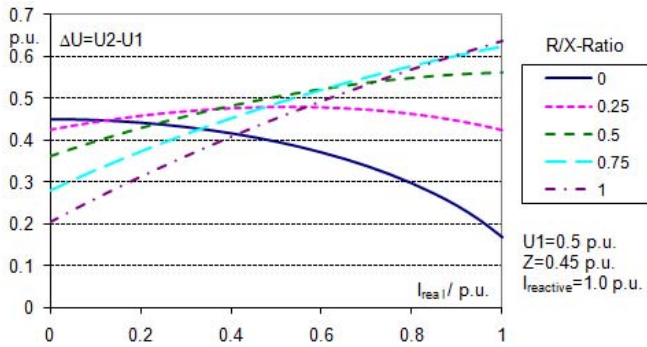


Fig. 16. Effect of active current injection on grid voltage.

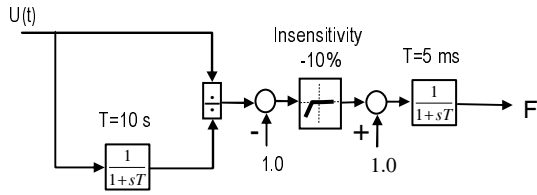


Fig. 17. Model of voltage dependent active current reduction.

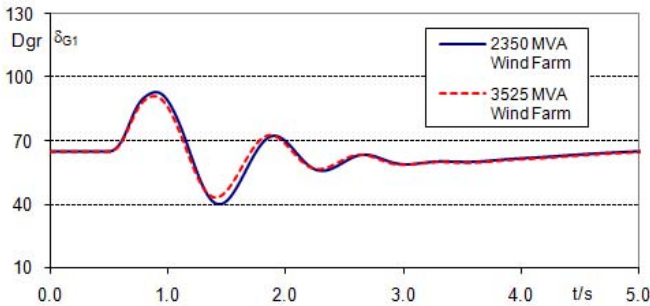


Fig. 18. Effect of voltage dependent active current reduction on the stability of G1.

IV. CONCLUSIONS

In this paper the effect of increased wind power generation on the transient stability performance of the interconnected system has been analyzed. Using real-world data both for the primary power equipments and controller parameters the swing curves of the conventional synchronous generators as well as the critical fault clearing times were computed for various scenarios involving different levels of wind integration. It was observed that while the electromechanical power oscillations, which typically occur following a grid fault in conventional synchronous generators, are not prevalent in wind generation plants, the overall impact of wind on the transient stability performance of the network, as exemplified by the critical fault clearing time, can be characterized as adverse. In fact, the CCT decreases as the share of wind in relation to the overall installed capacity increases.

The results of this simulation further reveal that the deadband in the voltage controller can cause oscillations in

voltage, real and reactive power. Considering the post fault transient performance of the system as the sole criterion, it can be stated that the system performs better without the deadband. It further follows from the results of the simulation that increasing the proportional gain (beyond the currently prescribed minimum of 2.0 in the German grid code) would significantly improve the transient stability performance of the system. In fact, the capability of the DFIG to support the network during and after a major grid fault by injecting adequate amount of reactive power into the PCC can be brought to a level comparable to that of the conventional synchronous generators or can even be surpassed.

Using a simplified model for the link between an offshore wind farm and the PCC, the adverse effect of the active current on the voltage support capability of the DFIG was illustrated. An extension to the DFIG control structure has been proposed, which reduces the real current when the voltage drop crosses a certain critical threshold. Using sample computations the capability of this approach to improve the transient stability behavior of the system has been demonstrated.

V. APPENDIX

Test power system and controller parameters

Line data:

| Component | Impedance | capacitance |
|----------------------|-------------------|-------------|
| 380-kV overhead line | 0.030+j0.266 Ω/km | 14.0 nF/km |
| 150-kV sub. cable | 0.046+j0.113 Ω/km | 241.0 nF/km |
| 33-kV sub. cable | 0.040+j0.110 Ω/km | 300.0 nF/km |

External network and load data:

| | |
|------------------|---------------------------------|
| External network | $Z_N = (1+j10) \Omega$ |
| Loads | $L1=L2=(1000+j100) \text{ MVA}$ |

Transformer data:

| Transformer type | Voltage | Rated power | Imp. |
|--------------------|-------------|-------------|------|
| Generator trafo | 15/400 kV | 500 MVA | 15% |
| 380/150 kV trafo | 380/150 kV | 470 MVA | 12% |
| 150/33 kV trafo | 150/31.5 kV | 470 MVA | 10% |
| Wind turbine trafo | 33/0.8 kV | 470 MVA | 8% |

Shunt Reactors:

| | |
|-----------------|-------------------------------|
| Offshore: 220 Ω | Onshore: 220-550 Ω (variable) |
|-----------------|-------------------------------|

Shunt capacitance:

| |
|---|
| $Q_c = 0 - 160 \text{ Mvar (variable)}$ |
|---|

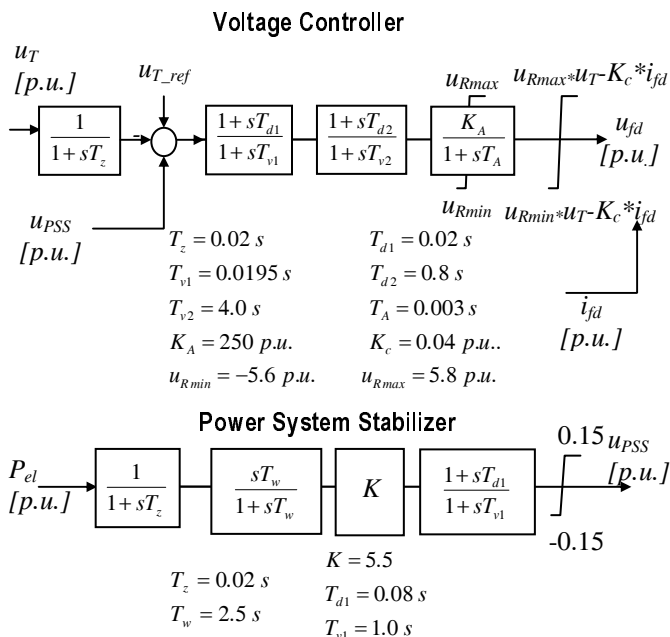
Fault Impedance:

| |
|--------------------------|
| $Z_F = (1.0+j10) \Omega$ |
|--------------------------|

Generator data (G1 and G2):

| | | |
|-------------------------|---------------------------|------------------------------|
| $S_n = 500 \text{ MVA}$ | $\cos \phi_n = 0.8$ | $U_n = 15 \text{ kV}$ |
| $T_m = 2H = 10s$ | $r_s = 0.01 \text{ p.u.}$ | $x_{GS} = 0.17 \text{ p.u.}$ |

| | | |
|---|-----------------------------|--------------------------|
| $T_d'' = 0.03 \text{ s}$ | $x_d'' = 0.21 \text{ p.u.}$ | $T_d' = 0.87 \text{ s}$ |
| $x_d' = 0.305 \text{ p.u.}$ | $x_d = 2.2 \text{ p.u.}$ | $T_q'' = 0.06 \text{ s}$ |
| $x_q'' = 0.23 \text{ p.u.}$ | $x_q = 2.0 \text{ p.u.}$ | |
| 5 th (reduced) order model has been used | | |



DFIG (values for the aggregated wind farm):

| | | |
|----------------------------------|----------------------------|------------------------------------|
| $U_n = 0.8 \text{ kV}$ | $S_n = 470 \text{ MVA}$ | $T_m = 2H = 7 \text{ s}$ |
| $P = 400 \text{ MW}$ | $r_s = 0.017 \text{ p.u.}$ | $x_{\sigma S} = 0.12 \text{ p.u.}$ |
| $x_m = 3.1 \text{ p.u.}$ | $r_R = 0.026 \text{ p.u.}$ | $x_{\sigma R} = 0.07 \text{ p.u.}$ |
| Definitions: | | |
| Synchronous speed = 1.0 p.u. | | |
| $\sigma = (1 - x_m^2 / x_R x_S)$ | $x_R = x_m + x_{\sigma R}$ | |
| $x_S = x_m + x_{\sigma S}$ | Slip $s = 1 - \omega_R$ | |

Rotor Side Controller:

| | | |
|---|---------------------------|--------------------------------|
| $T_1 = 0.005 \text{ s}$ | $K_I = 0.07 \text{ p.u.}$ | $T_I = 0.012 \text{ s}$ |
| $T_3 = 10 \text{ s}$ | $T_{ur} = 30 \text{ s}$ | $K_p = 2.5 - 7.5 \text{ p.u.}$ |
| Rotor current magnitude limitation: 1.35 p.u. | | |
| Stator voltage < 0.9 p.u. → rotor reactive current has priority, otherwise active current priority holds. | | |
| Rotor voltage magnitude limitation: 0.37 p.u. | | |
| Voltage controller deadband: $\pm 0.05 \text{ p.u.}$ | | |

Line Side Controller:

| | |
|---|---------------------------|
| $T_3 = 10 \text{ s}$ | $T_{L1} = 0.02 \text{ s}$ |
| LSC current magnitude limitation: 0.4 p.u. | |
| Always active current priority. | |
| DC link voltage is fixed at 1.0 p.u. | |
| $P_{RSC} = u_{Rd}^{\angle} i_{Rd}^{\angle} + u_{Rq}^{\angle} i_{Rq}^{\angle}$ | |

VI. REFERENCES

[1] I. Erlich, H. Wrede, and C. Feltes. "Dynamic Behavior of DFIG-Based Wind Turbines during Grid Faults". Power Conversion Conference - Nagoya, 2007. pp. 1195 – 1200.

- [2] I. Erlich, J. Kretschmann, J. Fortmann, S. Mueller-Engelhardt, and H. Wrede. "Modeling of Wind Turbines Based on Doubly-Fed Induction Generators for Power System Stability Studies". IEEE Transactions on Power Systems, Vol. 22, No. 3. Aug. 2007. pp. 909 - 919.
- [3] P. Kundur. "Power System Stability and Control". New York: Mc.Graw-Hill. 1994.
- [4] I. Erlich, "Analysis and simulation of dynamic behavior of power system", Postdoctoral lecture qualification, Dept. of electrical engineering, Dresden University, Germany, 1995
- [5] "Requirements for offshore grid connections in the E.on Netz Network" E.on Netz GmbH, Bayreuth, 1 April 2008, <http://www.eon-netz.com/Ressources/downloads/080702ENENAROS2008eng.pdf>
- [6] Erlich, I.; Kretschmann, J.; Fortmann, J.; Mueller-Engelhardt, S. & Wrede, H. Modeling of Wind Turbines Based on Doubly-Fed Induction Generators for Power System Stability Studies IEEE Transactions on Power Systems, 2007 Vol. 22 pp. 909-919
- [7] Y.Lei, A. Mullane, G. Lightbody, R. Yacimini, "Modeling of the Wind Turbine With a Doubly Fed Induction Generator for Grid Integration Studies", IEEE Trans. on Energy Conversion, vol. 21, pp. 257-264., March 2006
- [8] Ch. Eping, J. Stenzel, M. Pöller & H. Müller, "Impact of large scale wind power on power system stability", Fifth International Workshop on Large-Scale Integration of Wind Power and Transmission Networks for Offshore Wind Farms, Glasgow, Scotland, April 2005
- [9] A. Mullane, M. O'Malley, "The Inertial Response of Induction-Machine-Based Wind Turbines", IEEE Trans. Power Systems, vol. 20, pp. 1496-1503, Aug. 2005
- [10] F. M. Hughes, O. Anaya-Lara, N. Jenkins, G. Strbac, "Control of DFIG-Based Wind Generation for Power Network Support", IEEE Trans. Power Systems, vol. 20, pp. 1958-1966, Nov. 2005

VII. BIOGRAPHIES

Fekadu Shewarega (1956) received his Dipl.-Ing. Degree in electrical engineering from the Technical University of Dresden, Germany in 1985. From 1985 to 1988 he pursued his postgraduate studies in the same university and obtained his PhD degree in 1988. After graduation, he joined the Addis Ababa University, Ethiopia as the member of the academic staff where he served in various capacities. Currently he is a member of the research staff at the University Duisburg – Essen. His research interests are focused on power system analysis and renewable energy technologies.

Istvan Erlich (1953) received his Dipl.-Ing. degree in electrical engineering from the University of Dresden/Germany in 1976. After his studies, he worked in Hungary in the field of electrical distribution networks. From 1979 to 1991, he joined the Department of Electrical Power Systems of the University of Dresden again, where he received his PhD degree in 1983. In the period of 1991 to 1998, he worked with the consulting company EAB in Berlin and the Fraunhofer Institute IITB Dresden respectively. During this time, he also had a teaching assignment at the University of Dresden. Since 1998, he is Professor and head of the Institute of Electrical Power Systems at the University of Duisburg-Essen/Germany. His major scientific interest is focused on power system stability and control, modelling and simulation of power system dynamics including intelligent system applications. He is a member of VDE and IEEE.

José L. Rueda (GS'07) was born in 1980. He received the Electrical Engineer diploma from the Escuela Politécnica Nacional (EPN), Quito, Ecuador, in 2004. During 2004 he worked in Ecuador, in the field of electrical distribution networks operation and planning. Currently he is working toward the PhD degree at Instituto de Energía Eléctrica, Universidad Nacional de San Juan (IEE-UNSJ), Argentina, as part of scholarship financed by The German Academy Exchange Service (DAAD). Mr. Rueda is a graduate student member of the IEEE Power Engineering Society. His current research interests include power system stability and control, probabilistic and artificial intelligent methods, and wind farms.